Reduction of Mn19 Coordination Clusters on a Gold Surface

Jan Dreiser,*,[†,‡] Ayuk M. Ako,[§] Christian Wäckerlin,[†] Jakoba Heidler,[‡] Christopher E. Anson,[§] Annie K. Powell,[§,#] Cinthia Piamonteze,[‡] Frithjof Nolting,[‡] Stefano Rusponi,[†] and Harald Brune[†]

[†]Institute of Condensed Matter Physics, Ecole Polytechnique Fédérale de Lausanne, 1015 Lausanne, Switzerland

[‡]Swiss Light Source, Paul Scherrer Institut, 5232 Villigen PSI, Switzerland

[§]Institut für Anorganische Chemie, Karlsruhe Institute of Technology (KIT), 76131 Karlsruhe, Germany

[#]Institute of Nanotechnology, Karlsruhe Institute of Technology, Hermann-von-Helmholtz-Platz 1, 76344 Eggenstein-Leopoldshafen, Germany

Ⓢ *Supporting Information*

ABSTRACT: The magnetic properties of a Mn19 coordination cluster equipped with methylmercapto substituents on the organic ligands, $[Mn^{III}_{12}Mn^{II}_{7}(\mu_4\text{-}O)_8(\mu_3\text{-}Cl)_{7.7}(\mu_3\text{-}OMe)_{0.3}(HL^{SMe})_{12}(MeOH)_6]Cl_2\cdot27MeCN$ (Mn19(SMe)) (H_3L^{SMe} = 2,6-bis(hydroxymethyl)-4-mercapto-methylphenol) deposited on Au(111) surfaces from solution, have been investigated by X-ray absorption spectroscopy and X-ray magnetic circular dichroism. The data reveal that in the submonolayer regime the molecules contain only divalent Mn^{II} in contrast to the presence of Mn^{II} and Mn^{III} ions in the powder sample. Brillouin function fits to the field-dependent magnetization suggest that the total spin ground state in the submonolayer is much lower than S_{TOT} = 83/2 of the pristine molecules. These findings suggest that significant changes of the electronic structure, molecular geometry, and intramolecular exchange coupling take place upon surface deposition. A sample with coverage of 2−3 monolayers shows the presence of Mn^{III}, suggesting that a decoupling layer could stabilize the Mn19 core on a metallic surface.
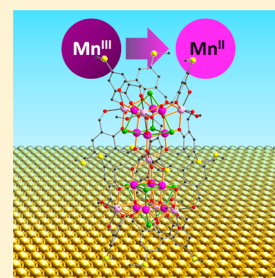
INTRODUCTION

Molecular nanomagnets are promising candidates for applications in molecular spintronics, high-density data storage, and quantum information processing.[1−5] A possible means to exploit their properties is to deposit them on surfaces such that they can be addressed one-by-one, e.g., by using a scanning tunneling microscope (STM) tip. Indeed, the surface deposition of molecular nanomagnets is an emerging focus in the field of molecular magnetism.[6−13] By using coordination cluster molecules as building blocks it is further possible to create new hybrid materials with properties that can be different from those of the molecules in the pristine, crystalline form.[14−19] To obtain a stable molecule−substrate system, it is useful to add functional end groups to the encapsulating ligands of coordination clusters which are suitable to attach the respective molecule to the surface of choice. Such functional end groups can be thiol groups and relatives forming covalent bonds with gold surfaces.[7,20−24] Chemisorption of molecules helps in the formation of monolayers because the adsorption energy of the first molecular layer on a substrate is significantly larger than that of the subsequent layers. Hence, it is possible to use wet chemistry which is well-suited for large molecules which cannot be sublimed because of their fragility.

Here we have chosen a member of the Mn19 family of spin clusters because of their robustness and their extraordinarily large spin ground states.[25−30] Furthermore, the trigonal symmetry within these molecules results in the canceling of the contributions of the individual Mn^{III} ion easy axes so that the molecules do not exhibit significant magnetic anisotro-

py.[24,27] This makes them ideal candidates in the search for a possible symmetry breaking as a result of surface deposition, i.e., for a surface-induced magnetic anisotropy. Recently, some of us have developed synthetic methodologies through which structurally related cluster systems displaying interesting topologies and/or exhibiting fascinating magnetic properties can be assembled.[26,27] Some of these synthetic advances have been employed in the preparation of Mn19(R) clusters. In the following, the abbreviation Mn19(R) refers to the respective Mn19 clusters without counterions and noncoordinated solvent molecules, with R the para-substituent on the phenolic organic ligands. Three different substituents are discussed in this work, R = {Me; OMe; SMe}, with "Me" denoting the methyl group. With surface deposition in mind, and within the framework of our continuing efforts to expand investigations on Mn19(R) systems, we prepared the recently reported cluster Mn19(SMe).[30] In designing our target compound we took note of the finding that the Mn19 clusters $[Mn^{III}_{12}Mn^{II}_{7}(\mu_4\text{-}O)_8(\mu_3\text{-}N_3)_8(HL^{Me})_{12}(MeCN)_6]Cl_2\cdot10MeOH\cdot MeCN$ [Mn19(Me)] (**1**, H_3L^{Me} = 2,6-bis(hydroxymethyl)-4-methyl-phenol) and $[Et_3NH]_2[Mn^{III}_{12}Mn^{II}_{7}(\mu_4\text{-}O)_8(\mu_3\text{-}N_3)_{7.4}(\mu_3\text{-}Cl)_{0.6}(HL^{OMe})_{12}(MeOH)_6]Cl_4\cdot14MeOH$ [Mn19(OMe)] (**2**, H_3L^{OMe} = 2,6-bis(hydroxymethyl)-4-methoxyphenol) can be adsorbed onto highly oriented pyrolytic graphite (HOPG) substrates. Mn19(Me) deposits as isolated single molecules, and

Mn_{19}(OMe) forms small groups of molecules at the step edges or at defects of the HOPG surfaces, and this was interpreted in terms of a degree of mobility of the clusters over the surface.[31] On the basis of these results, we assumed that replacement of the OMe ligand functionality in **2** by the sulfur-containing, closely isosteric (SMe) functionality might well be suitable for stabilizing the resulting Mn_{19}(SMe) on a Au(111) surface. The ligand 2,6-bis(hydroxymethyl)-4-methylmercaptophenol (H_3L^{SMe}), which has a methylmercapto functionality, was targeted because this end group promotes an interaction with the gold substrate that is weaker and more reversible than that of the corresponding thiophenol.[32−34]

We report herein on the X-ray absorption spectroscopy (XAS) and X-ray magnetic circular dichroism (XMCD)[35,36] characterization of the recently reported cluster $[Mn^{III}_{12}Mn^{II}_{7}(\mu_4\text{-O})_8(\mu_3\text{-Cl})_{7.7}(\mu_3\text{-OMe})_{0.3}(HL^{SMe})_{12}(MeOH)_6]Cl_2\cdot27MeOH$ **(3)**,[30] here abbreviated as Mn_{19}(SMe), adsorbed with different coverages on Au(111) surfaces (Figure 1). XAS and XMCD are receiving growing
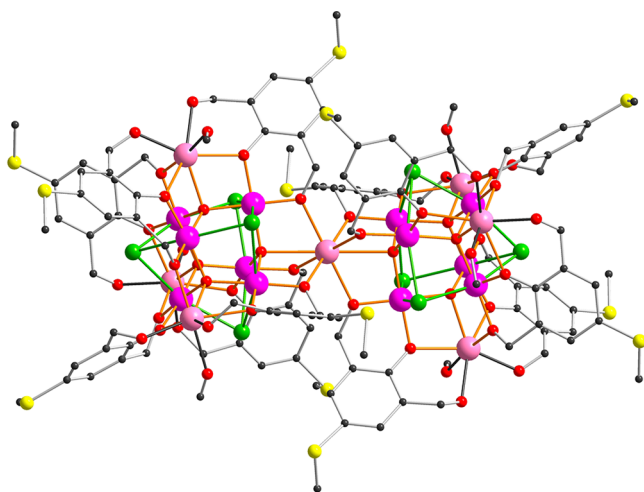

Figure 1. Molecular structure of **3** as obtained from X-ray diffraction.[30] Color code: Mn^{III}, purple; Mn^{II}, pink; O, red; Cl, green; S, yellow. The minor (methoxo) disorder component of the axial chloride ligands, chloride counterions, H atoms, and noncoordinated solvent molecules have been omitted for clarity.

interest because they allow the investigation of the magnetic properties of submonolayers of magnetic atoms and molecules on surfaces with elemental selectivity.[7,10,17,34,37,38] Whereas XAS gives information about oxidation states and ligand field, XMCD is sensitive to the magnetic moment localized at the element under investigation.

The structure of **3** consists of a central inorganic $\{Mn^{III}_{12}Mn^{II}_{7}(\mu_4\text{-O})_8\}$ core formed from the fusion of two supertetrahedral $\{Mn^{III}_6Mn^{II}_4\}$ units, in which the Mn^{II} centers describe the tetrahedra and share a common Mn^{II} vertex. Each of these tetrahedra has an octahedron of Mn^{III} centers inscribed within it linked by the $\mu_4\text{-O}^{2-}$ bridges. The temperature-dependent magnetic susceptibility $\chi(T)\cdot T$ and field-dependent magnetization $M(H)$ measurements of polycrystalline powder of **3** suggested a S_{TOT} = 83/2 ground state[30] similar to that of the parent compound **1**.[25] This spin ground state arises from ferromagnetic coupling of all of the manganese centers within the coordination cluster core of the molecule.

EXPERIMENTAL SECTION

To study the magnetic properties of surface-deposited Mn_{19}(SMe), we prepared three samples from solutions of **3** in MeOH and a polycrystalline powder sample of **3**. The sample descriptions are given in Table 1.

Table 1. Samples Used in the Present Study

sample	description
A	powder sample of **3**
B	substrate immersed in $c = 1.5 \times 10^{-5}$ M solution of **3** in MeOH
C	substrate immersed in $c = 1.5 \times 10^{-6}$ M solution of **3** in MeOH
D	substrate immersed in $c = 1.5 \times 10^{-7}$ M solution of **3** in MeOH

Au/Mica substrates (Phasis Sarl, Switzerland) were soaked overnight in 1.5×10^{-5} M, 1.5×10^{-6} M, and 1.5×10^{-7} M solutions of Mn_{19}(SMe) in methanol. Then the samples were rinsed with methanol and briefly dipped in an ultrasonic bath before being transferred into ultrahigh vacuum. Samples **B**, **C**, and **D** were mounted on the same sample holder. The powder sample **A** was prepared by pressing the polycrystalline powder of **3** into indium foil.

X-ray absorption spectra were measured at the X-Treme beamline line[39] (Swiss Light Source, Paul Scherrer Institut in collaboration with Ecole Polytechnique Fédérale de Lausanne) in total electron yield (TEY) mode at temperatures down to 6 K and magnetic fields up to 6.5 T. The beam was defocused (∼1 mm² diameter), and the X-ray flux was kept very low. Energy scans were measured at the Mn $L_{2,3}$ edges on-the-fly, that is, the monochromator and insertion device were moving continuously while the data was acquired.[40] Element-specific $M(H)$ curves were obtained by measuring the TEY at the energy of maximum dichroism (or at another energy specified in the main text) and at the pre-edge in an alternating fashion while ramping the magnetic field. Repeating this procedure for the two helicities of the X-rays and calculating the difference signal yielded the XMCD(H) curves shown in this work.

RESULTS AND DISCUSSION

The XAS recorded on samples **A**−**D** are shown in Figure 2. The X-ray spectra of the mixed-valent Mn ions at different sites superpose here, giving rise to rich spectral shapes. Whereas the Mn L_3 XAS of the powder sample (**A**) exhibits a comb of four distinct and strong features, virtually only two peaks are present for the lowest two concentrations (**C** and **D**). Sample **B** shows an intermediate behavior. Numerical calculations of the XAS based on a multiplet approach[41] in which the ligand field is parametrized by effective point charges suggest that the first (α) and part of the third (γ) peak can be attributed to Mn^{II}, whereas the second and fourth (β and δ, respectively) peaks result from Mn^{III}. Thus, the spectra shown in Figure 2 clearly indicate that the ratio of Mn^{II} versus Mn^{III} ions is greatly enhanced upon surface deposition, and in samples **C** and **D** all Mn^{III} have been reduced to Mn^{II}. It should be noted that photoreduction is absent because subsequent spectra do not show any change of the Mn XAS in time. While it is difficult to estimate the coverage with molecules by comparing the XAS of the powder and the surface-deposited molecules, a reasonable estimation of the molecular coverage can be achieved by comparing the Mn L_3 peak height versus pre-edge ratio with surface-deposited Mn-porphyrins.[42] The estimation yields 2.3, 0.5, and 0.14 monolayers for samples **B**, **C**, and **D**, respectively,
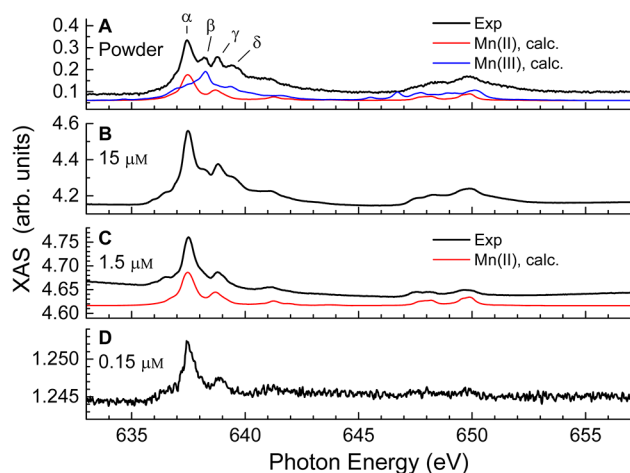
Figure 2. XAS at the Mn $L_{2,3}$ edges for samples **A−D**. $T = 6$ K and $\mu_0 H = -6.5$ T for **A−C**, and $T = 295$ K and $\mu_0 H = 0$ T for **D**. Colored lines indicate calculations for Mn^{II} (red) and Mn^{III} (blue) ions. Estimated coverages in monolayers: **B**, 2.3; **C**, 0.5; **D**, 0.14.

with one monolayer defined as a single close-packed layer of molecules. Because the similar cluster **1** has been shown to be redox-stable also in dilute solutions,[43] our results indicate that the interaction with the Au substrate must be responsible for the reduction to Mn^{II}.

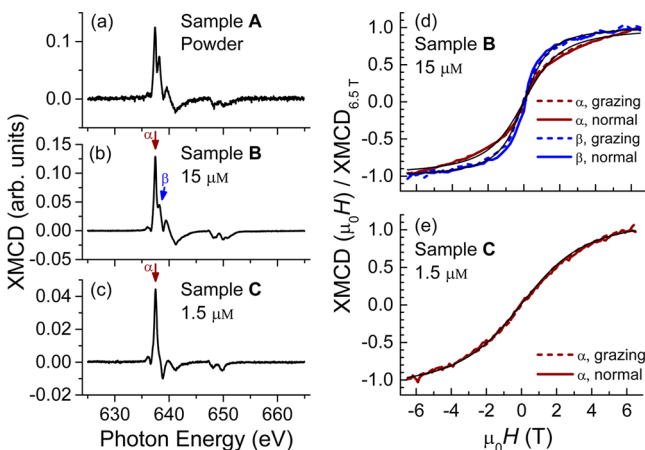The XMCD spectra measured on samples **A−C** are presented in Figure 3a−c. Clearly, these spectra reflect the

Figure 3. (a−c) XMCD of samples **A−C**, measured at −6.5 T in normal incidence of the X-rays ($\theta = 0°$). (d,e) $M(H)$ of samples **B** and **C** at normal and grazing incidence ($\theta = 60°$) of the X-rays obtained from the XMCD at peaks α and β at $E_\alpha = 637.5$ eV and $E_\beta = 638.25$ eV, respectively. Thin black lines indicate best-fit curves using the Brillouin function as described in the text. The temperature was 6 K for all measurements.

behavior of the XAS as seen in Figure 2, showing a trend toward reduction to Mn^{II} with decreasing concentrations and surface coverage. The sum rule analysis (cf. Supporting Information) reveals spin and orbital magnetic moments $M_s = 3.8 \pm 0.4\ \mu_B$ and $M_l = 0.4 \pm 0.1\ \mu_B$ in sample **C** with ∼0.5 monolayers coverage. In octahedral symmetry, $M_s = 5\ \mu_B$ and $M_l = 0\ \mu_B$ would be expected for Mn^{II}. The presence of an orbital magnetic moment therefore suggests a lowering of the ligand-field symmetry, which probably originates from surface-induced distortions.

The normalized $M(H)$ obtained from XMCD are depicted in Figure 3d,e for samples **B** and **C** at normal ($\theta = 0°$) and grazing ($\theta = 60°$) incidence of the X-rays, which probe the magnetic moment along the X-ray beam direction coinciding with the magnetic field direction. No hysteresis was observed; thus, the averages between backward and forward sweeps are shown. Because differences in the spectral weight of the Mn^{II} and Mn^{III} oxidation states were observed in the XMCD spectra of sample **B** (cf. Figure S2 of the Supporting Information), $M(H)$ was recorded at two X-ray energies. These energies correspond to the peaks α and β as indicated by arrows ($E_\alpha = 637.50$ eV and $E_\beta = 638.25$ eV) in Figure 3b,c. Indeed, the $M(H)$ curves obtained at the two peak energies are distinct in that the curve measured at E_β shows the onset of saturation but the curve measured on E_α does not. It should be noted that the responses, i.e., the TEY, from the first and second molecular layers in sample **B** are superposed in the two $M(H)$ measurements shown in Figure 3d because of the ∼5 nm sampling depth in TEY detection. The $M(H)$ measurements of samples **B** and **C** do not exhibit any angle dependence, i.e., no significant magnetic anisotropy is found. To obtain information about magnetic coupling between the Mn ions, we performed least-squares fits of the Brillouin function to the $M(H)$ curves shown in Figure 3d,e. In the fits, the temperature was fixed to that of the experiment ($T = 6$ K) and the total spin S_{TOT} was left free to vary. The Mn g-factor was fixed to $g = 2.0$. The fits revealed that $S_{TOT,\alpha} = 2.51 \pm 0.07$ in sample **C**, and $S_{TOT,\alpha} = 5.0 \pm 0.3$ and $S_{TOT,\beta} = 7.6 \pm 0.3$, corresponding to the XMCD measured on the α and β peaks, respectively, in sample **B**. The value for sample **C** corresponds to a magnetic moment of ∼5 μ_B, which is larger than the value of ∼4 μ_B extracted from sum rules. Thus, the total spin S_{TOT} value is much lower than that of the bulk compound in which $S_{TOT} = 83/2$.[25] Taking into account experimental errors and that the value ∼4 μ_B was obtained close to but not in full saturation, S_{TOT} of the submonolayer sample is, if at all, only slightly larger than the sum rule result. This could be explained either by a very weak ferromagnetic coupling between Mn^{II} ions or by mixed ferromagnetic−antiferromagnetic couplings almost compensating each other. Sample **B** displays larger values of S_{TOT}, with $S_{TOT,\beta} > S_{TOT,\alpha}$ because peak β probes mainly Mn^{III}, which is contained only in the second and higher layers as inferred from Figure 2. Thus, the magnetic properties of the molecules in the second layer appear to be closer to those of the pristine molecules, suggesting that in the second layer the Mn_{19} core could be present in the nondistorted, pristine form. As to the first layer, STM investigations described in the Supporting Information suggest that the molecules in the first layer are still structurally complete on the gold surface. The presence of different adsorption geometries is likely because of the nonflat three-dimensional shape of the Mn_{19} clusters and because of the presence of many anchoring sites given by the −SMe groups. From considerations of the molecular structure and S−Au bond formation, three possible adsorption geometries are proposed and depicted in the Supporting Information: In an upright geometry, $Mn_{19}(SMe)$ is bound to the surface via three thioether groups, and two side-on geometries can be identified involving three or four thioether groups. The presence of different adsorption geometries is corroborated by the rather large spreads observed in the area and apparent height histograms shown in Figure S4 of the Supporting Information. Note that on adsorption the orientation of the methyl part of −SMe can rotate about the bond between the S and the para

carbon atom on the aromatic ring, away from the positions taken in the molecular crystal.

Observations similar to those presented in this study were made in recent efforts to deposit monolayers of the Mn_{12} family on gold surfaces,[34,44−48] where a significant reduction of the magnetic core with respect to the pristine molecules was found when in direct contact with the metal. Among the reasons for the Mn reduction, there are (i) surface-to-molecule charge transfer, (ii) intramolecular charge reorganization, and (iii) partial loss of outer ligands. These effects may be linked to surface-induced molecular deformations, i.e., changes of the molecular structure on the surface, altogether leading to a concomitant change of the molecular electronic structure. These changes which take place on energy scales of electronvolts will have a significant effect on the intramolecular exchange coupling which is typically in the millielectronvolt energy range. The modification of the exchange coupling can therefore be considered as a secondary effect triggered by the reorganization of the molecular electronic structure. As mentioned before, our data indicate that indeed a surface-induced distortion of the Mn^{II} ligand field occurs. The decrease in the steepness of the magnetization $M(H)$ curves of the first layer of molecules demonstrates that a significant change of the magnetic properties upon surface deposition takes place, which must be related to the modifications of electronic structure, molecular geometry, and the subsequent alterations of the intramolecular magnetic exchange coupling. The presence of such modifications was also suggested by a recent density functional theory study.[49] Interestingly, the Mn reduction is almost absent in the Mn_6 single-molecule magnet when deposited on a Au(111) surface.[50] In view of the finding that the second layer of molecules is of mixed valence kind similar to the pristine molecules, the introduction of spacer molecules[44,51] or decoupling layers such as hexagonal boron nitride or graphene[52,53] could be a viable means of protecting the $Mn_{19}(SMe)$ molecules from reduction.

CONCLUSIONS

We have studied $Mn_{19}(SMe)$ as a powder sample and deposited on Au(111) surfaces from solutions of different concentrations by XAS and XMCD to investigate their chemical and magnetic properties. XAS indicates that the first molecular layer contains virtually only Mn^{II}, in contrast to the presence of Mn^{II} and Mn^{III} ions in the polycrystalline powder. In the second layer, the ratio of Mn^{II} and Mn^{III} ions is closer to that of the powder sample. This suggests a charge transfer from the metal surface, an intramolecular reorganization of charges, and/or a partial loss of ligands leading to a strong modification of the magnetic properties of the molecules. Brillouin fits to the field-dependent magnetization $M(H)$ reveal that in the submonolayer the total spin S_{TOT} is considerably lower than that of the pristine molecules. The Mn reduction found here is comparable to that reported in previous studies of surface-deposited Mn_{12} single-molecule magnets.

ASSOCIATED CONTENT

ⓢ Supporting Information

Details of XAS and XMCD of samples **B** and **C**, STM results. This material is available free of charge via the Internet at http://pubs.acs.org.

AUTHOR INFORMATION

Corresponding Author

*E-mail: jan.dreiser@epfl.ch.

Notes

The authors declare no competing financial interest.

ACKNOWLEDGMENTS

REFERENCES

(1) Leuenberger, M. N.; Loss, D. Quantum Computing in Molecular Magnets. *Nature* **2001**, *410*, 789−793.

(2) Rocha, A. R.; García-Suárez, V. M.; Bailey, S. W.; Lambert, C. J.; Ferrer, J.; Sanvito, S. Towards Molecular Spintronics. *Nat. Mater.* **2005**, *4*, 335−339.

(3) Troiani, F.; Ghirri, A.; Affronte, M.; Carretta, S.; Santini, P.; Amoretti, G.; Piligkos, S.; Timco, G.; Winpenny, R. E. P. Molecular Engineering of Antiferromagnetic Rings for Quantum Computation. *Phys. Rev. Lett.* **2005**, *94*, 207208.

(4) Bogani, L.; Wernsdorfer, W. Molecular Spintronics Using Single-Molecule Magnets. *Nat. Mater.* **2008**, *7*, 179−186.

(5) Timco, G. A.; Carretta, S.; Troiani, F.; Tuna, F.; Pritchard, R. J.; Muryn, C. A.; McInnes, E. J. L.; Ghirri, A.; Candini, A.; Santini, P.; et al. Engineering the Coupling between Molecular Spin Qubits by Coordination Chemistry. *Nat. Nanotechnol.* **2009**, *4*, 173−178.

(6) Gatteschi, D.; Cornia, A.; Mannini, M.; Sessoli, R. Organizing and Addressing Magnetic Molecules. *Inorg. Chem.* **2009**, *48*, 3408−3419.

(7) Mannini, M.; Pineider, F.; Sainctavit, P.; Danieli, C.; Otero, E.; Sciancalepore, C.; Talarico, A. M.; Arrio, M.-A.; Cornia, A.; Gatteschi, D.; et al. Magnetic Memory of a Single-Molecule Quantum Magnet Wired to a Gold Surface. *Nat. Mater.* **2009**, *8*, 194−197.

(8) Margheriti, L.; Mannini, M.; Sorace, L.; Gorini, L.; Gatteschi, D.; Caneschi, A.; Chiappe, D.; Moroni, R.; de Mongeot, F. B.; Cornia, A.; et al. Thermal Deposition of Intact Tetrairon(III) Single-Molecule Magnets in High-Vacuum Conditions. *Small* **2009**, *5*, 1460−1466.

(9) Rancan, M.; Sedona, F.; Marino, M. D.; Armelao, L.; Sambi, M. Chromium Wheels Quasi-Hexagonal 2D Assembling by Direct UHV Sublimation. *Chem. Commun. (Cambridge, U.K.)* **2011**, *47*, 5744−5746.

(10) Gonidec, M.; Biagi, R.; Corradini, V.; Moro, F.; De Renzi, V.; del Pennino, U.; Summa, D.; Muccioli, L.; Zannoni, C.; Amabilino, D. B.; et al. Surface Supramolecular Organization of a Terbium(III) Double-Decker Complex on Graphite and Its Single Molecule Magnet Behavior. *J. Am. Chem. Soc.* **2011**, *133*, 6603−6612.

(11) Domingo, N.; Bellido, E.; Ruiz-Molina, D. Advances on Structuring, Integration and Magnetic Characterization of Molecular Nanomagnets on Surfaces and Devices. *Chem. Soc. Rev.* **2011**, *41*, 258−302.

(12) Cornia, A.; Mannini, M. Single-Molecule Magnets on Surfaces. *Struct. Bonding (Berlin, Ger.)* **2014**, 1−38.

(13) Lorusso, G.; Jenkins, M.; González-Monje, P.; Arauzo, A.; Sesé, J.; Ruiz-Molina, D.; Roubeau, O.; Evangelisti, M. Surface-Confined Molecular Coolers for Cryogenics. *Adv. Mater. (Weinheim, Ger.)* **2013**, *25*, 2984−2988.

(14) Scheybal, A.; Ramsvik, T.; Bertschinger, R.; Putero, M.; Nolting, F.; Jung, T. A. Induced Magnetic Ordering in a Molecular Monolayer. *Chem. Phys. Lett.* **2005**, *411*, 214−220.

(15) Wende, H.; Bernien, M.; Luo, J.; Sorg, C.; Ponpandian, N.; Kurde, J.; Miguel, J.; Piantek, M.; Xu, X.; Eckhold, P.; et al. Substrate-

Induced Magnetic Ordering and Switching of Iron Porphyrin Molecules. *Nat. Mater.* **2007**, *6*, 516−520.

(16) Bogani, L.; Cavigli, L.; Gurioli, M.; Novak, R. L.; Mannini, M.; Caneschi, A.; Pineider, F.; Sessoli, R.; Clemente-León, M.; Coronado, E.; et al. Magneto-Optical Investigations of Nanostructured Materials Based on Single-Molecule Magnets Monitor Strong Environmental Effects. *Adv. Mater. (Weinheim, Ger.)* **2007**, *19*, 3906−3911.

(17) Gambardella, P.; Stepanow, S.; Dmitriev, A.; Honolka, J.; de Groot, F. M. F.; Lingenfelder, M.; Gupta, S. S.; Sarma, D. D.; Bencok, P.; Stanescu, S.; et al. Supramolecular Control of the Magnetic Anisotropy in Two-Dimensional High-Spin Fe Arrays at a Metal Interface. *Nat. Mater.* **2009**, *8*, 189−193.

(18) Rogez, G.; Donnio, B.; Terazzi, E.; Gallani, J.-L.; Kappler, J.-P.; Bucher, J.-P.; Drillon, M. The Quest for Nanoscale Magnets: The Example of [Mn$_{12}$] Single Molecule Magnets. *Adv. Mater. (Weinheim, Ger.)* **2009**, *21*, 4323−4333.

(19) Lodi Rizzini, A.; Krull, C.; Balashov, T.; Kavich, J. J.; Mugarza, A.; Miedema, P. S.; Thakur, P. K.; Sessi, V.; Klyatskaya, S.; Ruben, M.; et al. Coupling Single Molecule Magnets to Ferromagnetic Substrates. *Phys. Rev. Lett.* **2011**, *107*, 177205.

(20) Nuzzo, R. G.; Allara, D. L. Adsorption of Bifunctional Organic Disulfides on Gold Surfaces. *J. Am. Chem. Soc.* **1983**, *105*, 4481−4483.

(21) Corradini, V.; Moro, F.; Biagi, R.; De Renzi, V.; del Pennino, U.; Bellini, V.; Carretta, S.; Santini, P.; Milway, V. A.; Timco, G.; et al. Successful Grafting of Isolated Molecular Cr$_7$Ni Rings on Au(111) Surface. *Phys. Rev. B: Condens. Matter Mater. Phys.* **2009**, *79*, 144419.

(22) Corradini, V.; Ghirri, A.; del Pennino, U.; Biagi, R.; Milway, V. A.; Timco, G.; Tuna, F.; Winpenny, R. E. P.; Affronte, M. Grafting Molecular Cr$_7$Ni Rings on a Gold Surface. *Dalton Trans.* **2010**, *39*, 4928.

(23) Rodriguez-Douton, M. J.; Mannini, M.; Armelao, L.; Barra, A.-L.; Tancini, E.; Sessoli, R.; Cornia, A. One-Step Covalent Grafting of Fe$_4$ Single-Molecule Magnet Monolayers on Gold. *Chem. Commun. (Cambridge, U.K.)* **2011**, *47*, 1467−1469.

(24) Ghirri, A.; Corradini, V.; Bellini, V.; Biagi, R.; del Pennino, U.; De Renzi, V.; Cezar, J. C.; Muryn, C. A.; Timco, G. A.; Winpenny, R. E. P.; et al. Self-Assembled Monolayer of Cr$_7$Ni Molecular Nanomagnets by Sublimation. *ACS Nano* **2011**, *5*, 7090−7099.

(25) Ako, A. M.; Hewitt, I. J.; Mereacre, V.; Clérac, R.; Wernsdorfer, W.; Anson, C. E.; Powell, A. K. A Ferromagnetically Coupled Mn$_{19}$ Aggregate with a Record *S* = 83/2 Ground Spin State. *Angew. Chem., Int. Ed.* **2006**, *45*, 4926−4929.

(26) Ako, A. M.; Mereacre, V.; Clerac, R.; Wernsdorfer, W.; Hewitt, I. J.; Anson, C. E.; Powell, A. K. A [Mn$_{18}$Dy] SMM Resulting from the Targeted Replacement of the Central Mn^{II} in the *S* = 83/2 [Mn$_{19}$]-Aggregate with Dy^{III}. *Chem. Commun. (Cambridge, U.K.)* **2009**, 544−546.

(27) Ako, A. M.; Burger, B.; Lan, Y.; Mereacre, V.; Clérac, R.; Buth, G.; Gómez-Coca, S.; Ruiz, E.; Anson, C. E.; Powell, A. K. Magnetic Interactions Mediated by Diamagnetic Cations in [Mn$_{18}$M] (M = Sr^{2+}, Y^{3+}, Cd^{2+}, and Lu^{3+}) Coordination Clusters. *Inorg. Chem.* **2013**, *52*, 5764−5774.

(28) Waldmann, O.; Ako, A. M.; Güdel, H. U.; Powell, A. K. Assessment of the Anisotropy in the Molecule Mn$_{19}$ with a High-Spin Ground State *S* = 83/2 by 35 GHz Electron Paramagnetic Resonance. *Inorg. Chem.* **2008**, *47*, 3486−3488.

(29) Ge, C.-H.; Ni, Z.-H.; Liu, C.-M.; Cui, A.-L.; Zhang, D.-Q.; Kou, H.-Z. Nonadecanuclear Cluster with a Spin Ground State of *S* = 73/2. *Inorg. Chem. Commun.* **2008**, *11*, 675−677.

(30) Mameri, S.; Ako, A. M.; Yesil, F.; Hibert, M.; Lan, Y.; Anson, C. E.; Powell, A. K. Coordination Cluster Analogues of the High-Spin [Mn$_{19}$] System with Functionalized 2,6-Bis(hydroxymethyl)phenol Ligands. *Eur. J. Inorg. Chem.* **2014**, *2014*, 4326−4334.

(31) Ako, A. M.; Alam, M. S.; Mameri, S.; Lan, Y.; Hibert, M.; Stocker, M.; Müller, P.; Anson, C. E.; Powell, A. K. Adsorption of [Mn$_{19}$] Aggregates with *S* = 83/2 onto HOPG Surfaces. *Eur. J. Inorg. Chem.* **2012**, *2012*, 4131−4140.

(32) Lavrich, D. J.; Wetterer, S. M.; Bernasek, S. L.; Scoles, G. Physisorption and Chemisorption of Alkanethiols and Alkyl Sulfides on Au(111). *J. Phys. Chem. B* **1998**, *102*, 3456−3465.

(33) Zobbi, L.; Mannini, M.; Pacchioni, M.; Chastanet, G.; Bonacchi, D.; Zanardi, C.; Biagi, R.; Pennino, U. D.; Gatteschi, D.; Cornia, A.; et al. Isolated Single-Molecule Magnets on Native Gold. *Chem. Commun. (Cambridge, U.K.)* **2005**, 1640−1642.

(34) Mannini, M.; Sainctavit, P.; Sessoli, R.; Cartier dit Moulin, C.; Pineider, F.; Arrio, M.-A.; Cornia, A.; Gatteschi, D. XAS and XMCD Investigation of Mn$_{12}$ Monolayers on Gold. *Chem.—Eur. J.* **2008**, *14*, 7530−7535.

(35) Stöhr, J. Exploring the Microscopic Origin of Magnetic Anisotropies with X-Ray Magnetic Circular Dichroism (XMCD) Spectroscopy. *J. Magn. Magn. Mater.* **1999**, *200*, 470−497.

(36) Funk, T.; Deb, A.; George, S. J.; Wang, H.; Cramer, S. P. X-Ray Magnetic Circular Dichroism—A High Energy Probe of Magnetic Properties. *Coord. Chem. Rev.* **2005**, *249*, 3−30.

(37) Rau, I. G.; Baumann, S.; Rusponi, S.; Donati, F.; Stepanow, S.; Gragnaniello, L.; Dreiser, J.; Piamonteze, C.; Nolting, F.; Gangopadhyay, S.; et al. Reaching the Magnetic Anisotropy Limit of a 3*d* Metal Atom. *Science* **2014**, *344*, 988−992.

(38) Wäckerlin, C.; Chylarecka, D.; Kleibert, A.; Müller, K.; Iacovita, C.; Nolting, F.; Jung, T. A.; Ballav, N. Controlling Spins in Adsorbed Molecules by a Chemical Switch. *Nat. Commun.* **2010**, *1*, 61.

(39) Piamonteze, C.; Flechsig, U.; Rusponi, S.; Dreiser, J.; Heidler, J.; Schmidt, M.; Wetter, R.; Calvi, M.; Schmidt, T.; Pruchova, H.; et al. X-Treme Beamline at SLS: X-Ray Magnetic Circular and Linear Dichroism at High Field and Low Temperature. *J. Synchrotron Radiat.* **2012**, *19*, 661−674.

(40) Krempaský, J.; Flechsig, U.; Korhonen, T.; Zimoch, D.; Quitmann, C.; Nolting, F. Synchronized Monochromator and Insertion Device Energy Scans at SLS. *AIP Conf. Proc.* **2010**, *1234*, 705−708.

(41) Uldry, A.; Vernay, F.; Delley, B. Systematic Computation of Crystal-Field Multiplets for X-Ray Core Spectroscopies. *Phys. Rev. B: Condens. Matter Mater. Phys.* **2012**, *85*, 125133.

(42) Wäckerlin, C.; Tarafder, K.; Siewert, D.; Girovsky, J.; Hählen, T.; Iacovita, C.; Kleibert, A.; Nolting, F.; Jung, T. A.; Oppeneer, P. M.; et al. On-Surface Coordination Chemistry of Planar Molecular Spin Systems: Novel Magnetochemical Effects Induced by Axial Ligands. *Chem. Sci.* **2012**, *3*, 3154−3160.

(43) Ako, A. M.; Lan, Y.; Hampe, O.; Cremades, E.; Ruiz, E.; Anson, C. E.; Powell, A. K. All-Round Robustness of the Mn$_{19}$ Coordination Cluster System: Experimental Validation of a Theoretical Prediction. *Chem. Commun. (Cambridge, U.K.)* **2014**, *50*, 5847−5850.

(44) Voss, S.; Fonin, M.; Rüdiger, U.; Burgert, M.; Groth, U.; Dedkov, Y. S. Electronic Structure of Mn$_{12}$ Derivatives on the Clean and Functionalized Au Surface. *Phys. Rev. B: Condens. Matter Mater. Phys.* **2007**, *75*, 045102.

(45) Voss, S.; Burgert, M.; Fonin, M.; Groth, U.; Rudiger, U. A Comparative Study on the Deposition of Mn$_{12}$ Single Molecule Magnets on the Au(111) Surface. *Dalton Trans.* **2008**, 499−505.

(46) Grumbach, N.; Barla, A.; Joly, L.; Donnio, B.; Rogez, G.; Terazzi, E.; Kappler, J.-P.; Gallani, J.-L. Loss of Single-Molecule-Magnet Behavior of a Mn$_{12}$-Based Compound Assembled in a Monolayer. *Eur. Phys. J. B* **2010**, *73*, 103−108.

(47) Saywell, A.; Magnano, G.; Satterley, C. J.; Perdigão, L. M. A.; Britton, A. J.; Taleb, N.; del Carmen Giménez-López, M.; Champness, N. R.; O'Shea, J. N.; Beton, P. H. Self-Assembled Aggregates Formed by Single-Molecule Magnets on a Gold Surface. *Nat. Commun.* **2010**, *1*, 75.

(48) Saywell, A.; Britton, A. J.; Taleb, N.; Giménez-López, M.; del, C.; Champness, N. R.; Beton, P. H.; O'Shea, J. N. Single Molecule Magnets on a Gold Surface: In Situ Electrospray Deposition, X-Ray Absorption and Photoemission. *Nanotechnology* **2011**, *22*, 075704.

(49) Totti, F.; Rajaraman, G.; Iannuzzi, M.; Sessoli, R. Computational Studies on SAMs of {Mn$_6$} SMMs on Au(111): Do Properties Change upon Grafting? *J. Phys. Chem. C* **2013**, *117*, 7186−7190.

(50) Moro, F.; Corradini, V.; Evangelisti, M.; Biagi, R.; De Renzi, V.; del Pennino, U.; Cezar, J. C.; Inglis, R.; Milios, C. J.; Brechin, E. K. Addressing the Magnetic Properties of Sub-Monolayers of Single-Molecule Magnets by X-Ray Magnetic Circular Dichroism. *Nanoscale* **2010**, *2*, 2698−2703.

(51) Otero, G.; Evangelio, E.; Rogero, C.; Vázquez, L.; Gómez-Segura, J.; Gago, J. A. M.; Ruiz-Molina, D. Morphological Investigation of Mn_{12} Single-Molecule Magnets Adsorbed on Au(111). *Langmuir* **2009**, *25*, 10107−10115.

(52) Kahle, S.; Deng, Z.; Malinowski, N.; Tonnoir, C.; Forment-Aliaga, A.; Thontasen, N.; Rinke, G.; Le, D.; Turkowski, V.; Rahman, T. S.; et al. The Quantum Magnetism of Individual Manganese-12-Acetate Molecular Magnets Anchored at Surfaces. *Nano Lett.* **2012**, *12*, 518−521.

(53) Järvinen, P.; Hämäläinen, S. K.; Banerjee, K.; Häkkinen, P.; Ijäs, M.; Harju, A.; Liljeroth, P. Molecular Self-Assembly on Graphene on SiO_2 and H-BN Substrates. *Nano Lett.* **2013**, *13*, 3199−3204.